Measurement of $p\bar{p} \rightarrow ZZ \rightarrow \ell^+\ell^-\ell'^+\ell'^-$ production cross section using RunIIb Data

The DØ Collaboration
URL http://www-d0.fnal.gov
(Dated: July 25, 2008)

We present an analysis of Z boson pair production decaying into $eeee$, $\mu\mu\mu\mu$ and $ee\mu\mu$ with approximately 1.7 fb^{-1} of RunIIb data. The total number of events expected from $p\bar{p} \rightarrow ZZ \rightarrow \ell^+\ell^-\ell'^+\ell'^-$ signal in all three decay modes is 2.13 ± 0.08 events whereas $0.14^{+0.03}_{-0.02}$ event is expected from background processes (stat.+syst.). We observe 3 candidate events in our data. The probability of observation in the background-only hypothesis is 4.33×10^{-8} which corresponds to a significance of 5.3 standard deviations. The measured cross section is $\sigma(p\bar{p} \rightarrow ZZ) = 1.75^{+1.27}_{-0.86}(stat.) \pm 0.08(syst.) \pm 0.10(lumi)$ pb. This value is consistent with the Standard Model expectation of 1.60 pb.

Preliminary Results for Summer 2008 Conferences

I. INTRODUCTION

Measurement of the pair production rates for electroweak gauge bosons at the Fermilab Tevatron provides important tests of experimental and theoretical methods employed in the search for the Higgs boson. The standard model (SM) predicts a cross section times branching fraction $\sigma \times BF < 100$ fb for the all charged lepton final state $ZZ \to \ell\ell\ell'\ell'$, with $\ell, \ell' = e$ or μ. This small cross section, which approaches that for Higgs boson production for some possible Higgs masses, has prevented verification of ZZ production rates at a hadron collider up until recently, when dramatic improvements in Tevatron luminosity have opened the possibility of direct observation. Further, as ZZ production in the SM cannot occur through direct ZZZ or $ZZ\gamma^*$ couplings, an observation of unexpectedly high cross section could provide evidence for anomalous interactions between neutral gauge bosons [1]. The D0 detector is especially well-suited for detecting $ZZ \to \ell\ell\ell'\ell'$, owing to its excellent electron and muon identification over a wide range of lepton rapidities.

Previous analyses of ZZ production have been performed at Tevatron $p\bar{p}$ and LEP e^+e^- Colliders. The D0 collaboration reported a $ZZ \to \ell\ell\ell'\ell'$ search with 1 fb^{-1} of data that resulted in a 95% C.L. limit of $\sigma(ZZ) < 4.4$ pb on the production cross section [2]. The analysis also yielded limits on anomalous trilinear ZZZ and $ZZ\gamma^*$ couplings. The CDF collaboration reported a signal for ZZ production at 4.4 σ significance from combined $ZZ \to \ell\ell\ell'\ell'$ and $ZZ \to \ell\ell\nu\nu$ searches, and measured a production cross section of $\sigma(ZZ) = 1.4^{+0.7}_{-0.6}$ pb [3]. In this Letter, we present a new search for ZZ production with charged leptonic decays of both Z bosons decaying into electron or muon pairs. This leads to four electron ($eeee$), four muons ($\mu\mu\mu\mu$), and two electron-two muon ($ee\mu\mu$) final states.

Data used in this analysis were collected with the D0 detector at the Fermilab Tevatron $p\bar{p}$ Collider at $\sqrt{s} = 1.96$ TeV in the period between June 2006 and April 2008. The integrated luminosities [4] of the three channels are approximately 1.7 fb^{-1} each and are shown in Table I.

II. DETECTOR

A brief description of the main components of the D0 Run II detector [5] important to this analysis follows. The central-tracking system of the D0 detector consists of a silicon microstrip tracker (SMT) and a central fiber tracker (CFT), both located within a 2 T solenoidal magnetic field. The SMT has a six-barrel longitudinal structure, each with a set of four layers arranged axially around the beam pipe, and interspersed with 16 radial disks. It provides tracking and vertexing capability up to pseudorapidity $|\eta| \simeq 3.0$. The CFT has eight thin coaxial barrels, each supporting two doublets of overlapping scintillating fibers, one doublet parallel to the collision axis, and the other alternating by $\pm 3°$ relative to the axis. The CFT provides full coverage up to $|\eta| \simeq 1.6$. A liquid argon and uranium calorimeter has a central section (CC) covering pseudorapidities $|\eta|$ up to ≈ 1.1, and two end calorimeters (EC) that extend coverage to $|\eta| \approx 4.2$, with all three housed in separate cryostats [7]. The calorimeters are segmented along the shower direction with four layers comprising electromagnetic (EM) section and an additional three to five layers forming the hadronic section. This allows for electron-pion separation based on longitudinal and transverse shower shape. A muon system [8] resides beyond the calorimetry, and consists of a layer of tracking detectors and scintillation trigger counters before 1.8 T toroids, followed by two similar layers after the toroids. Tracking at $|\eta| < 1$ relies on 10 cm wide drift tubes [7], while 1 cm mini-drift tubes are used at $1 < |\eta| < 2$. Luminosity is measured using plastic scintillator arrays located in front of the EC cryostats, covering $2.7 < |\eta| < 4.4$ [4].

The D0 detector uses a three level (L1, L2 and L3) trigger system. Electrons candidates are required to have energy deposition in the EM section of the calorimeter at L1 and L2. At L3, a requirement is applied on the fraction of energy in the EM calorimeter and on shower shape. The L1 muon trigger requires hits in the muon scintillation counters and a match with a track in the L1 track system. At L2, muon candidates are required to have track segments in the muon tracking detectors, and a minimum transverse momentum (p_T). At L3, some muons are also required to have a matched track from the inner tracker.

III. SELECTION

This analysis employs a combination of single electron and di-electron triggers for the $eeee$ channel. Similarly, single muon and di-muon triggers are used for the $\mu\mu\mu\mu$ channel. The $ee\mu\mu$ channel uses a combination of all these triggers, plus additional electron-muon triggers. The triggering efficiency for events with four high-p_T leptons that satisfy all other selection requirements exceeds 99%.

For the $eeee$ channel, the four electrons must have transverse energies $E_T > 30, 20, 15,$ and 15 GeV, respectively. Electrons must be reconstructed either in the CC region of $|\eta| < 1.1$ or in the EC region of $1.5 < |\eta| < 3.2$, and be isolated from other energy clusters. Electrons in the CC are required to satisfy identification criteria based on a

multivariate discriminant derived from calorimeter shower shape and a matched track reconstructed in the SMT and CFT. Electrons in the EC are not required to have a matched track, but must satisfy more stringent shower shape requirements. At least two electrons must be in the CC region. With no requirement applied on the charge of the electrons, three possible Z combinations can be formed for each $eeee$ event. Events are required to have at least one Z with a di-electron invariant mass above 70 GeV and the other above 50 GeV. Finally, events are split into three categories depending on the number of electrons in the CC region: events with two CC electrons, with three CC electrons and with $\geq$ four CC electrons. These are subsequently referred to as $eeee_{2CC}$, $eeee_{3CC}$, and $eeee_{4CC}$, respectively. The three sub-samples suffer from significantly different levels of background contamination while being mutually exclusive.

For the $\mu\mu\mu\mu$ channel, each muon must satisfy quality criteria based on scintillator and wire chamber information from the muon system and have a matched track in the inner tracker. The four most energetic muons need to satisfy transverse momentum requirements $p_T > 30, 25, 15$, and 15 GeV, respectively. At least three muons in the event must be isolated, each passing a requirement of less than 2.5 GeV of transverse energy deposited in the calorimeter in an annulus between $R = 0.1$ and $R = 0.4$ centered around the muon track [9]. This reduces backgrounds from $Z \to \ell\ell$+jets and $t\bar{t}$ production where at least two of the four muons usually originate from semileptonic b- and c-quark decays, and are therefore surrounded by significant energy deposition in the calorimeter. Finally, the distance in the transverse plane of closest approach to the beam spot for the track matched to the muon must be less than 0.02 cm for tracks with SMT hits and less than 0.2 cm for tracks without SMT hits. This reduces the background from muons that do not originate from the primary vertex such as those from b decays and cosmic rays. The maximum distance between the muon track vertices for all muon pairs along the beam axis is required to be less than 3 cm. This reduces backgrounds from muons produced by beam particle interactions outside of the D0 detector and cosmic ray muons. Of the three possible ZZ combinations per event that can be formed without considering muon charge, at least one Z is required to have the di-muon invariant mass above 70 GeV and the other above 50 GeV.

For the $ee\mu\mu$ channel, the two most energetic electrons and muons must satisfy the conditions $E_T > 20, 15$ GeV, respectively, for the electrons, and $p_T > 20, 15$ GeV, respectively, for the muons. All muons and electrons must satisfy the single lepton selection criteria defined for the $eeee$ and $\mu\mu\mu\mu$ final states. In addition, electrons and muons are required to be spatially separated by $R > 0.2$ to reduce backgrounds from final states such as single $Z \to \mu\mu$ production in which both muons are accompanied by radiated photons. At least one muon must satisfy the same calorimeter isolation requirement imposed in the $\mu\mu\mu\mu$ final state. This requirement reduces the background from $Z \to ee$+jets and $t\bar{t}$ production where muons usually originate from semileptonic b- and c-quark decays, and are therefore are not isolated. One pair of the same flavor leptons must have invariant mass greater than 70 GeV, while the other pair is required to have invariant mass greater than 50 GeV. Finally, events are split into three categories depending on the number of electrons in the CC region: events with no CC electron, with one CC electron and with $\geq$ two CC electrons. These are refereed to as $ee\mu\mu_{0CC}$, $ee\mu\mu_{1CC}$ and $ee\mu\mu_{2CC}$ sub-samples, respectively. As in the four electron channel, these sub-samples suffer from significantly different levels of background contamination.

IV.   SIGNAL AND BACKGROUND MODELING

Monte Carlo (MC) simulations determine the expected number of signal events in each sub-channel. The MC uses the PYTHIA event generator [10], with an assumed cross section of $\sigma(ZZ) = 1.6 \pm 0.1$ pb [11]. It then incorporates the integrated luminosities computed separately for each sub-sample, taking into account data quality criteria, and performs a detailed GEANT-based simulation [12] of the detector response, employing the same reconstruction software as for data. Finally, data-derived reconstruction and identification efficiencies for single electrons and muons, obtained from large samples of $Z \to ee$ and $Z \to \mu\mu$ events are used. Table I summarizes the results for expected signal, including systematic uncertainties from the lepton identification/reconstruction efficiencies, energy/momentum resolutions, and the signal modeling.

The backgrounds to $ZZ \to \ell\ell\ell'\ell'$ signal arise from $(Z \to \ell\ell) +$ jets and $(Z \to \ell\ell) + \gamma +$ jets events, and from top quark pair production ($t\bar{t}$). Production of $Z +$ jets events with leptonic decays of $Z \to \ell\ell$ can lead to an $\ell\ell\ell'\ell'$ final state when the jets are either mis-identified as electrons or muons, or contain real electrons or muons from in-flight decays of pions, kaons, or heavy-flavored hadrons. In $(Z \to \ell\ell) + \gamma +$ jets production the additional two leptons can come from a photon passing electron identification criteria and from a jet mimicking an electron. To estimate the $Z + \gamma +$ jets background, we first measure the probability for a jet to produce an electron or muon that satisfy the identification criteria. The probability for a jet to misreconstruct as an electron was measured in di-jet events selected via jet triggers, using electron candidates that satisfy all selection criteria except the isolation condition $R < 0.5$ to the nearest jet. Lower-E_T jets that contain an electron within $R < 0.5$ are considered to mimic an electron. The probability for a jet to mimic an electron is parameterized in terms of the jet E_T and η. It is $\sim 4 \times 10^{-4}$ for the case of CC electrons which are required to have a matched track, and $\sim 5 \times 10^{-3}$ in the case of EC electrons for which no

TABLE I: The integrated luminosity, expected number of signal and background events, and the number of observed candidates in the seven $ZZ \to \ell\ell\ell'\ell'$ subchannels (stat.+syst.)

Subchannel	$eeee_{2CC}$	$eeee_{3CC}$	$eeee_{4CC}$	$\mu\mu\mu\mu$	$ee\mu\mu_{0CC}$	$ee\mu\mu_{1CC}$	$ee\mu\mu_{2CC}$
Luminosity (fb^{-1})	1.75±0.11	1.75±0.11	1.75±0.11	1.68±0.10	1.68±0.10	1.68±0.10	1.68±0.10
Signal	0.094±0.005	0.194±0.006	0.158±0.006	0.60±0.05	0.065±0.007	0.39±0.04	0.62±0.05
$Z(\gamma)$+jets bkgd.	$0.030^{+0.009}_{-0.008}$	$0.018^{+0.008}_{-0.007}$	$0.002^{+0.002}_{-0.001}$	$0.0003^{+0.0001}_{-0.0001}$	$0.03^{+0.02}_{-0.01}$	0.05 ± 0.01	$0.008^{+0.004}_{-0.003}$
$t\bar{t}$ background	–	–	–	–	$0.0012^{+0.0016}_{-0.0009}$	0.005 ± 0.002	$0.0007^{+0.0009}_{-0.0005}$
Observed events	0	0	2	1	0	0	0

track matching requirement is applied. The probability for a jet to produce a muon was measured in a di-jet sample using a procedure similar to that described for electrons where the higher E_T jet is called the tag jet, and the lower E_T jet is the probe jet. This probability is parameterized in terms of the tag jet E_T and probe jet η. The probability for a 15 GeV (100 GeV) jet to produce a muon of $p_T > 15$ GeV is $\sim 10^{-4}(10^{-2})$ when no muon isolation requirement is applied, and it is $\sim 10^{-5}(10^{-4})$ when the muon is required to be isolated. A systematic uncertainty of 30% is assigned to account for observed variations in the probabilities when changing selection criteria of the di-jet events used for misidentification determination for the leptons.

The probabilities for jets to be misidentified as electrons are then applied to the jets in $eee +$ jets and $\mu\mu e +$ jets data to determine the background for the $eeee$ and $ee\mu\mu$ channels, respectively. This method takes into account contributions from $Z +$ jets, $Z + \gamma +$ jets, $WZ +$ jets, $WW +$ jets, $W +$ jets and ≥ 4 jets. However, it double counts contribution from $Z +$ two jets where an event can be selected as an $eee/\mu\mu e +$ jet candidate if either of the two jets mimic an electron, whereas it can only contribute to $eeee$ or $\mu\mu ee$ sample if both jets mimic an electron. To correct for the double counting, $ee/\mu\mu +$ two jets events are used, with the electron misidentification probabilities applied to both jets. The $ee/\mu\mu$+jets rates is subtracted from the $eee/\mu\mu e+$ jets rates to obtain the final background estimate. The probabilties for jets to contain a muon are applied to the jets in $\mu\mu +$ two jets data to determine the background estimate for the $\mu\mu\mu\mu$ channel. Systematic uncertainties on this background arise from the 30% uncertainty in measured misreconstruction rates, and from the limited statistics of the data remaining in the samples after selection cuts.

The background from $t\bar{t}$ events is estimated via the same method as described previously for the signal MC. A theoretical cross section of $\sigma^{NNLL}(t\bar{t}) =7.9$ pb [13] assuming $m_{top} = 170$ GeV was used. The systematic uncertainty on the $t\bar{t}$ background includes a 10% theory uncertainty on $\sigma(t\bar{t})$, as well as the contributions from the normalization and acceptance variation originating from the top quark mass uncertainty.

V. RESULTS

Table I summarizes background contributions to each sub-channel. The total expected number of candidates from background sources is $0.14^{+0.03}_{-0.02}$ event. The sub-channels with the lowest expected background contamination are $eeee_{4CC}$ and $\mu\mu\mu\mu$, where the expected number of background events are $0.002^{+0.002}_{-0.001}$ and $0.0003^{+0.0001}_{-0.0001}$, respectively. We observe a total of three candidates in our data, two in the $eeee_{4CC}$ subchannel and one in the $\mu\mu\mu\mu$ channel. Table II summarizes the candidates' kinematic characteristics. Figure 1 shows the distribution of the four lepton invariant mass for the data candidates and for the expected signal and background events.

We extract statistical significance of the observed fluctuation using a negative log-likelihood ratio (LLR) test-statistic method. As input, we use the expected yields from the signal and the background, separated into the seven subchannels. A modified frequentistic method is used [14] that returns the probability (p-value) of background-only fluctuating to give the observed yield or higher. The resulting LLR distribution combined across all seven subchannels for the RunIIb data set is shown in Figure 5 of the Appendix. In 3×10^8 background-only pseudo-experiments, we observe 13 with an LLR value smaller or equal to that observed in data. This gives a p-value of 4.33×10^{-8} that corresponds to a 5.3σ standard deviation significance. Minimizing the LLR function yields a measured cross section of $\sigma(p\bar{p} \to ZZ) = 1.75^{+1.27}_{-0.86}(stat.) \pm 0.08(syst.) \pm 0.10(lumi)$ pb, consistent with standard model expectations.

TABLE II: Characteristics of the observed candidate events.

		e_1^+	e_2^+	e_3^-	e_4^-
eeee candidate 1	p_T (GeV)	107.4	59.1	52.2	16.5
	η_D	0.72	0.25	-0.58	-0.79
		$e_1^+ e_4^-$		$e_2^+ e_3^-$	
	dimass (GeV)	89.4		60.9	
	Z p_T (GeV)	110.2		106.1	
	$\not{E}_T$ (GeV)	3.4			
		e_1^+	e_2^+	e_3^-	e_4^-
eeee candidate 2	p_T (GeV)	82.6	74.7	34.8	26.5
	η_D	0.48	0.24	0.74	1.07
		$e_1^+ e_3^-$		$e_2^+ e_4^-$	
	dimass (GeV)	99.3		90.1	
	Z p_T (GeV)	63.8		58.1	
	$\not{E}_T$ (GeV)	18.4			
		μ_1^+	μ_2^-	μ_3^-	μ_4^+
$\mu\mu\mu\mu$ candidate	p_T (GeV)	115.5	77.5	42.1	24.0
	η_D	0.02	-0.98	0.80	-1.89
		$\mu_1^+ \mu_3^-$		$\mu_2^- \mu_4^+$	
	dimass (GeV)	147.6		89.8	
	Z p_T (GeV)	79.9		62.4	
	$\not{E}_T$ (GeV)	2.8			
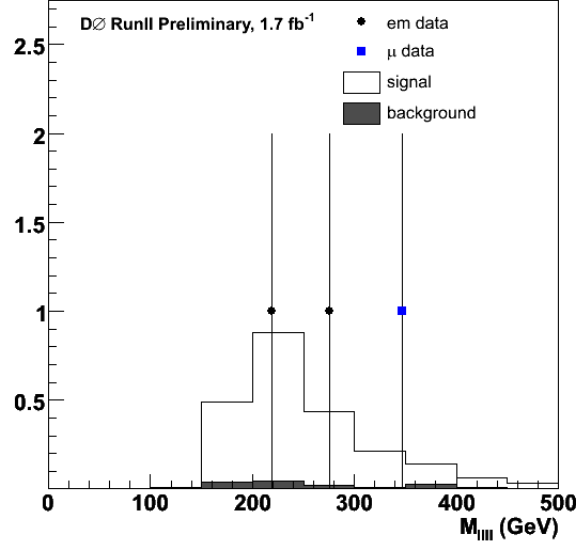
FIG. 1: Distribution of four-lepton invariant mass in data, expected signal, and expected background events for a cross section of 1.6 pb.

VI. ACKNOWLEDGEMENTS

---

[a] Visitor from Augustana College, Sioux Falls, SD, USA.
[b] Visitor from The University of Liverpool, Liverpool, UK.
[c] Visitor from ICN-UNAM, Mexico City, Mexico.
[d] Visitor from II. Physikalisches Institut, Georg-August-University, Göttingen, Germany.
[e] Visitor from Helsinki Institute of Physics, Helsinki, Finland.
[f] Visitor from Universität Zürich, Zürich, Switzerland.
[‡] Deceased.

[1] U. Baur and D. Rainwater, Phys. Rev. D **62**, 113011 (2000).
[2] DØ Collaboration, B. Abbott *et al.*, Phys. Rev. Lett. **100**, 131801 (2008).
[3] CDF Collaboration, T. Aaltonen *et al.*, arXiv:0801.4806v1.
[4] T. Andeen *et al.*, FERMILAB-TM-2365 (2007).
[5] DØ Collaboration, V. Abazov *et al.*, Nucl. Instrum. Methods (Phys. Res.) A **565**, 463 (2006).
[6] The D0 coordinate system is cylindrical with the z-axis along the proton beamline and the polar and azimuthal angles denoted as θ and ϕ respectively. The pseudorapidity is defined as $\eta = -\ln \tan(\theta/2)$.
[7] DØ Collaboration, S. Abachi *et al.*, Nucl. Instrum. Methods (Phys. Res.) A **338**, 185 (1994).
[8] V. M. Abazov *et al.*, Nucl. Instrum. Meth. A **552**, 372 (2005) [arXiv:physics/0503151].
[9] The variable R between two objects i and j is defined as $R = \sqrt{(\eta_i - \eta_j)^2 + (\phi_i - \phi_j)^2}$.
[10] T. Sjöstrand *et al.*, Comput. Phys. Commun. **135**, 238 (2001).
[11] J. M. Campbell and R. K. Ellis, Phys. Rev. D **60**, 113006 (1999) [arXiv:hep-ph/9905386].
[12] R. Brun and F. Carminati, CERN Program Library Long Writeup W5013, 1993 (unpublished).
[13] N. Kidonakis and R. Vogt, Phys. Rev. D **68**, 114014 (2003) [arXiv:hep-ph/0308222].
[14] W.Fisher, FERMILAB-TM-2386-E (2007).

APPENDIX A: ADDITIONAL PLOTS

Run 231347 Evt 25076242 Wed Mar 14 08:32:56 2007
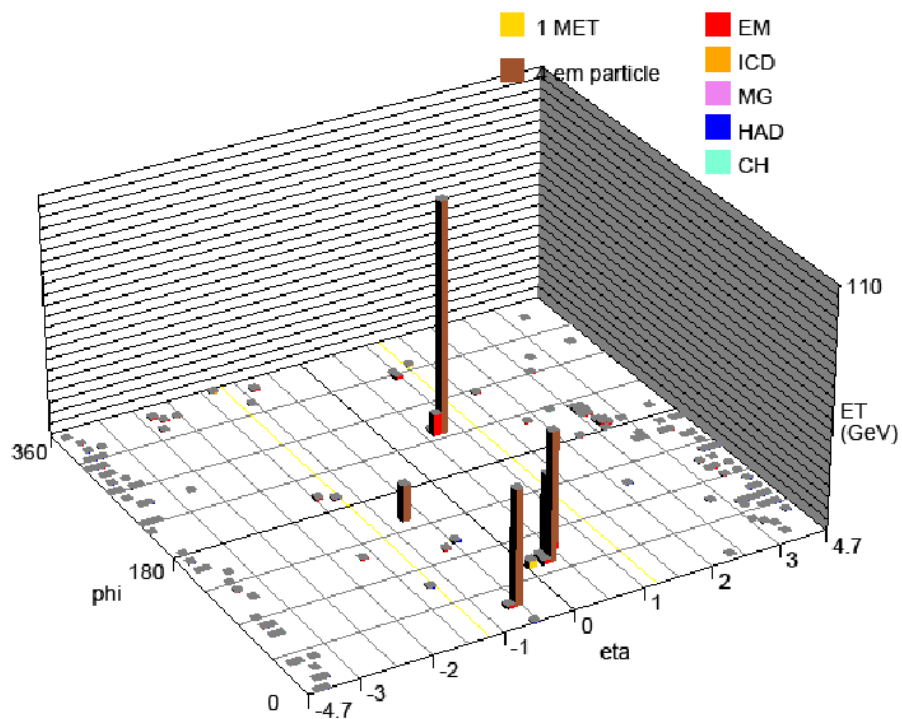
Run 231347 Evt 25076242 Wed Mar 14 08:32:56 2007
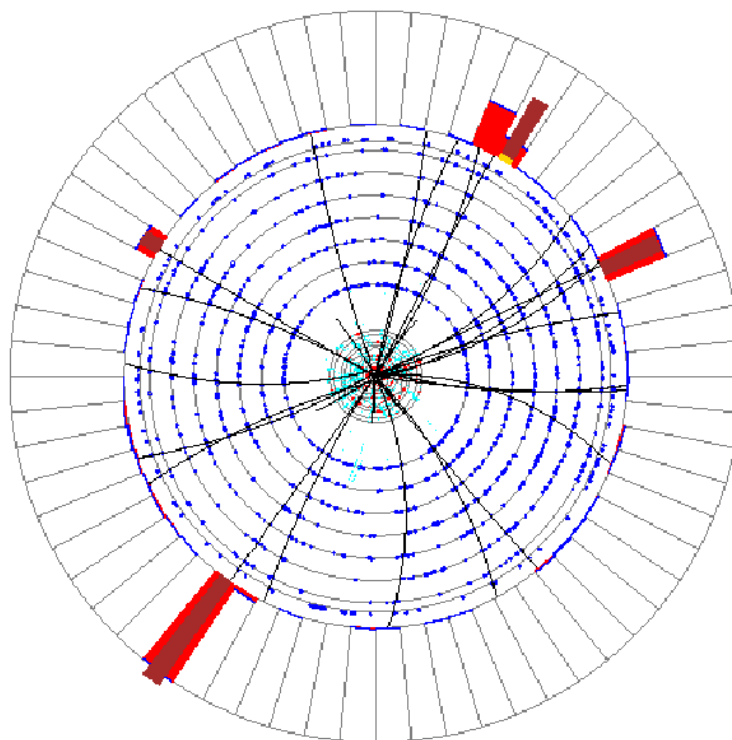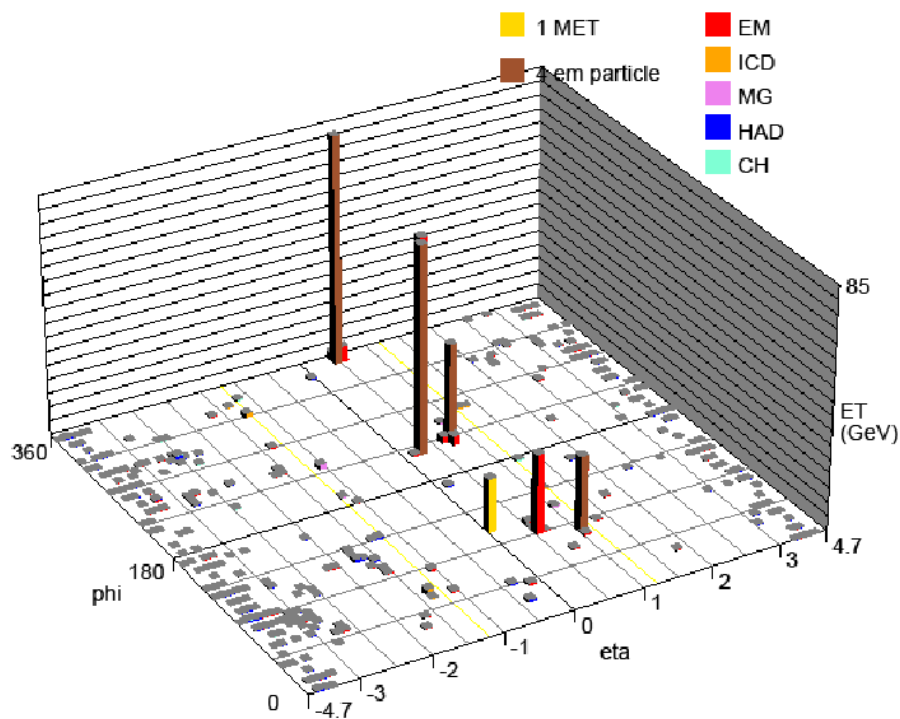
ET scale: 98 GeV

FIG. 2: Event display for *eeee* candidate 1.

Run 223736 Evt 14448774 Sun Jul 30 07:03:38 2006
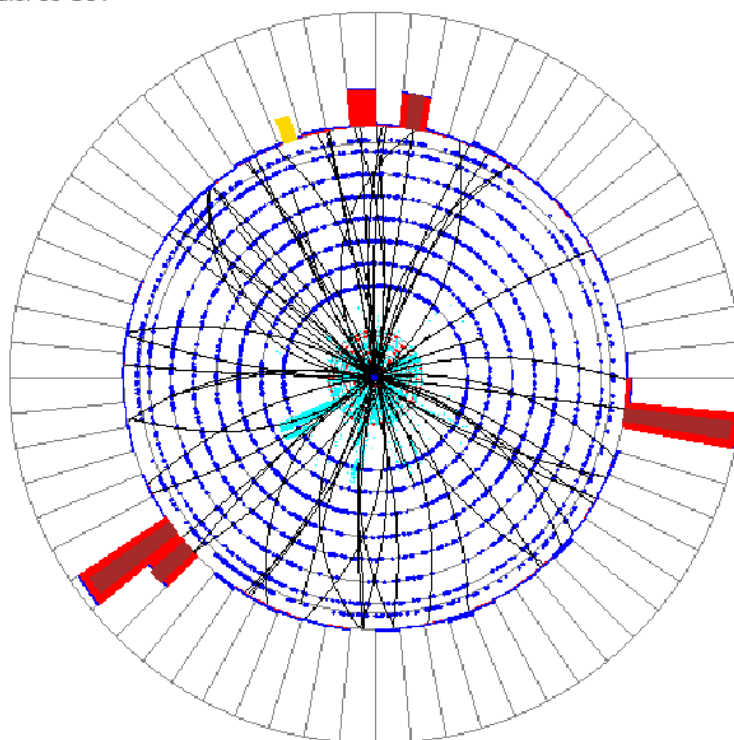
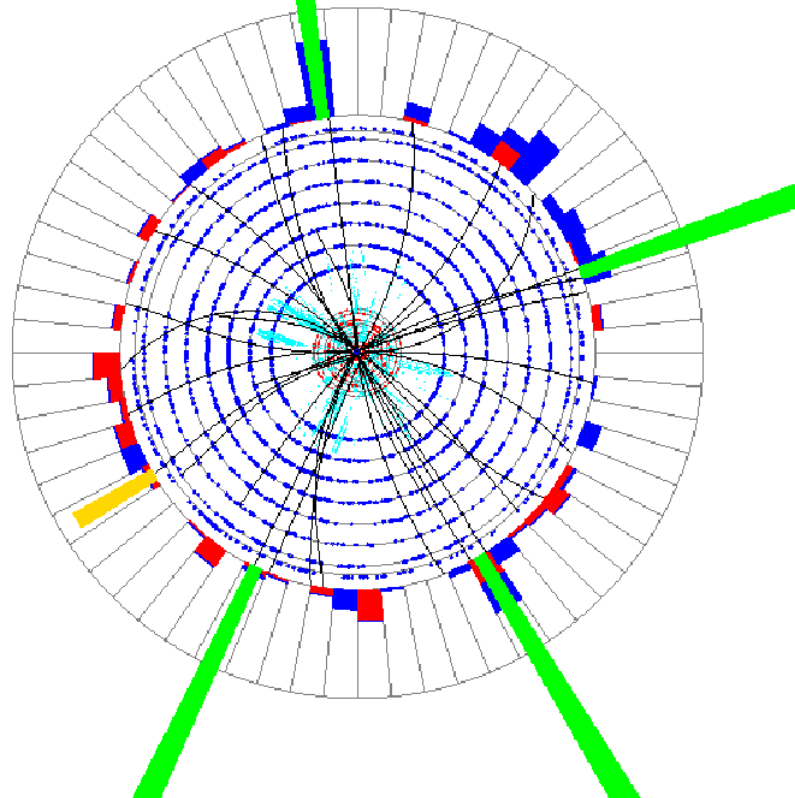FIG. 3: Event display for *eeee* candidate 2.

Run 232216 Evt 15136574 Mon Apr 16 12:01:04 2007

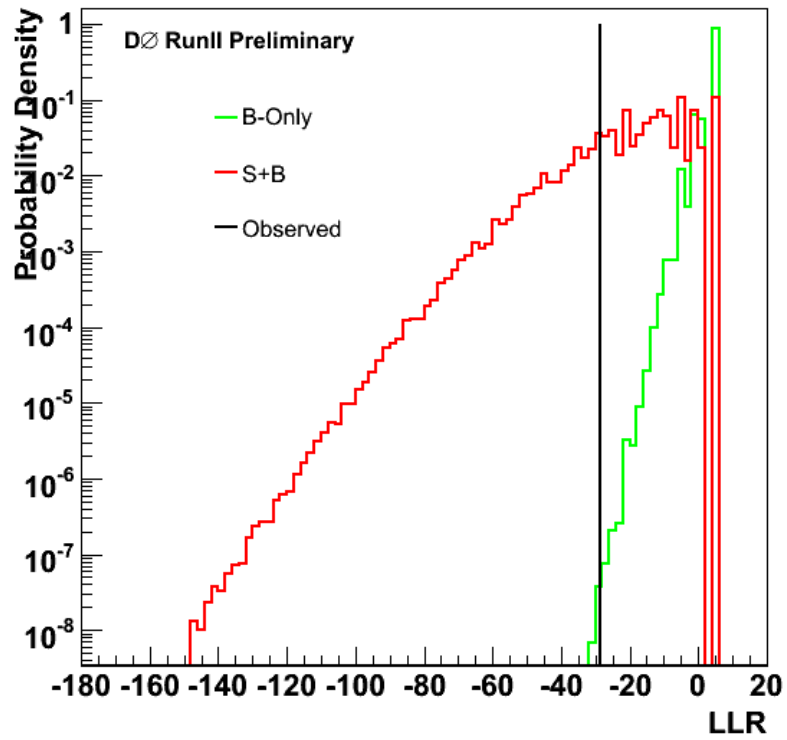FIG. 4: Event display for $\mu\mu\mu\mu$ candidate.

FIG. 5: LLR distribution in many pseudo-experiments for the signal plus background (S+B) and background only (B only) hypothesis combining the seven subchannels for the RunIIb data set. Observation is shown by the solid line
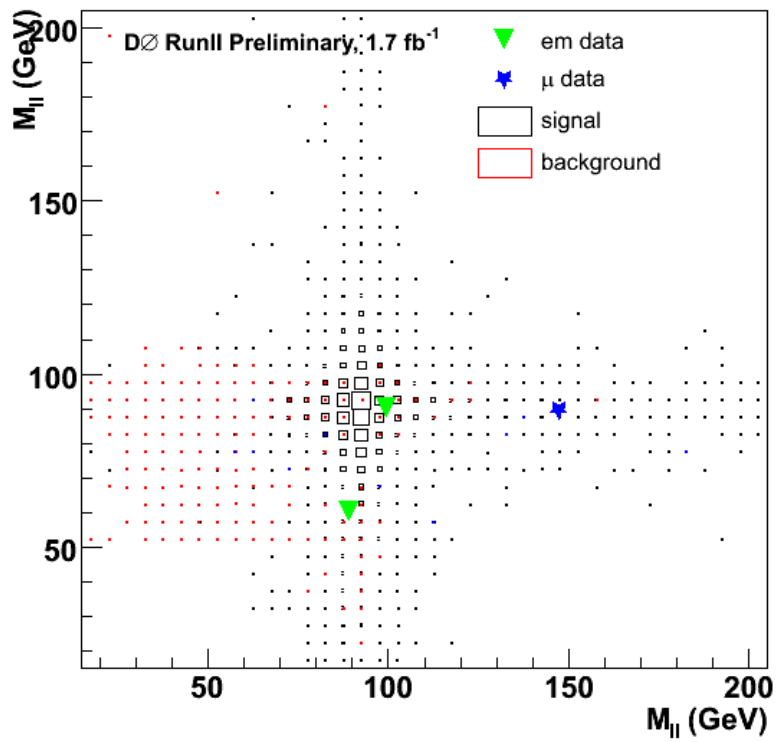
FIG. 6: Dilepton mass pairing in data, expected signal and background.